Biophysical Chemistry, 38 (1990) 213–224
Elsevier

BIOCHE 01504

Optical absorption spectra of azurin and stellacyanin in glycerol / water and ethylene glycol / water solutions in the temperature range 290–20 K

Antonio Cupane, Maurizio Leone, Eugenio Vitrano and Lorenzo Cordone

Istituto di Fisica dell'Università and GNSM-CISM, Via Archirafi, 36-90123, Palermo, Italy

Received 20 November 1989
Revised manuscript received 23 April 1990
Accepted 24 April 1990

Azurin; Stellacyanin; Optical spectroscopy; Low temperature; Protein stereodynamics

We have measured the optical absorption spectra of azurin and stellacyanin in the wavelength range 1100–350 nm and in the temperature interval 290—20 K. Samples are protein aqueous solutions containing 65% (v/v) glycerol or ethylene glycol as cryoprotectants and remain homogeneous and transparent throughout the whole temperature range investigated. Spectra are deconvoluted into Gaussian components and the temperature dependence of the zeroth, first and second moments of the various bands is analyzed, within the harmonic Franck-Condon approximation, to obtain information on the stereodynamic properties of the active sites of these proteins. Sizable differences of the integrated intensities of all the bands with temperature are observed and are attributed to variations of the metal-ligand relative positions (i.e., deformations of the active site) that occur as the temperature is lowered. The mean effective frequency of the nuclear vibrations coupled to all the observed bands is about 150 cm^{-1} for both proteins in both solvents used; this indicates that the electronic transitions from which the optical spectrum originates are substantially coupled with low-frequency vibrational modes, likely ligand-metal-ligand deformations. The relevance of the stereodynamic properties of azurin and stellacyanin, investigated in this work, to their functional behavior is also suggested.

1. Introduction

The optical absorption bands of a chromophore embedded in a crystalline matrix exhibit half-width narrowing and peak position shift as the temperature is lowered. This effect is due to the interaction of the optical electrons with the vibrations of nearby atoms of the crystalline lattice. The theory, developed several years ago to study the optical properties of color centers in crystals [1–3], assumes that the electron-lattice interaction depends quadratically upon the displacement of the nuclei from their equilibrium positions and makes use of the Franck-Condon approximation; it can be shown that the temperature dependence of the first (M_1) and second (M_2) moment of an absorption band can be expressed as [1,4]:

$$M_1 = \Delta E/h + 2\pi^2/h\Sigma_j S_j R_j \nu_j(\mathrm{g}) + 1/4\Sigma_j (R_j - 1)\nu_j(\mathrm{g}) \coth\left[h\nu_j(\mathrm{g})/2kT\right] \quad (1a)$$

$$M_2 = 2\pi^2/h\Sigma_j S_j R_j^2 \nu_j^2(\mathrm{g}) \coth\left[h\nu_j(\mathrm{g})/2kT\right] + I^2 \quad (1b)$$

where k and h denote Boltzmann's and Planck's constants, respectively; ΔE is the energy difference between the excited and ground electronic states when the nuclei are in their equilibrium positions; S_j and R_j are the Franck-Condon linear and quadratic coupling constants of the j-th normal mode with the electronic transition; $\nu_j(\mathrm{g})$

Correspondence address: A. Cupane, Istituto di Fisica dell' Università and GNSM-CISM, Via Archirafi, 36-90123, Palermo, Italy.

is the frequency of the j-th normal mode when the electron is in the ground state; the sums are extended over the entire set $\{j\}$ of normal modes to which the electronic transition under consideration is coupled; the term I^2 in the M_2 expression takes into account the presence of temperature-independent halfwidth contributions due to the finite lifetime of the excited electronic state (homogeneous broadening).

Eqs 1 are not useful in analyzing experimental data since, in general, independent measurements of ν_j, S_j and R_j are not available. For this reason the following approximate expressions, obtained from eqs 1 by taking the average over the normal modes, are widely used:

$$M_1 = D + F \coth[h\nu/2kT] \tag{2a}$$

$$M_2 = A \coth[h\nu/2kT] + C^2 \tag{2b}$$

where the parameter ν is a 'mean effective' frequency of the nuclear motions coupled to the electronic transition. The term I^2 is now included in the parameter C^2 together with contributions arising from the coupling with high-frequency modes not populated in the temperature range investigated; the analogous contributions to M_1 are included in the parameter D.

If the sample is composed of a great number of species which are spectrally heterogeneous (inhomogeneous broadening), the parameter ΔE in eq. 1a has to be considered as an average value; moreover, the sums in eqs 1 are to be extended not only over the normal modes, but also over all the species present. Optical spectra are not affected by the interconversion between species (motional narrowing), since at all temperatures interconversion times are much slower than the characteristic times of electronic transitions. It is easy to imagine that the effect of heterogeneity does not alter the behavior of M_1 (eq. 2a), whereas it adds to M_2 a contribution that is temperature-independent if the distribution of spectrally heterogeneous species does not depend upon temperature, and that therefore can be included in the term C^2.

In a recent series of papers [5–8], it has been shown that eqs. 2 can also be applied to rationalize the temperature dependence of the optical spectra of a chromophore embedded in a protein matrix; in particular, the liganded and unliganded derivatives of ferrous hemoglobin and myoglobin have been studied in detail. This has allowed relevant information to be obtained on the local dynamic properties of these proteins in the proximity of the heme group and on the electron-vibration coupling constants, as well as on their dependence upon the protein structure and the composition of the external medium.

In this work we have applied the approach described above to analyze the temperature dependence of the optical absorption spectra of azurin and stellacyanin. These two proteins belong to the class of so-called 'blue copper proteins' [9]; their biological function is to act as electron-transfer agents in the respiratory chain of some bacteria or in the photosynthetic system of a number of plants. The active site is characterized by a single Cu^{2+} coordinated to four (or five) atoms from side chains of amino acid residues of the protein; the particular coordination geometry gives rise to a peculiar absorption spectrum in the visible region characterized by a very intense central band at about 600 nm (responsible for the beautiful blue color of these proteins) and by two much weaker lateral bands, one on the ultraviolet and the other on the near-infrared side. This spectrum is usually assigned to charge-transfer transitions from orbitals of the liganded atoms to the copper $d_{x^2-y^2}$ orbital. The analysis of the temperature dependence of the optical spectrum is therefore a useful tool for investigating the dynamic properties of these proteins in the proximity of the active site; in turn, due to the intimate structure-dynamics-function interconnection, this will also add to the understanding of their functional behavior.

2. Materials and methods

Azurin (from *Pseudomonas aeruginosa*) was purchased from Sigma and was used without further purification. Stellacyanin (from *Rhus vernicifera*) was a kind gift from Prof. B. Salvato and was purified according to the procedure described in ref. 10. For azurin, the ratio A(280 nm)/A(625

nm), measured at 290 K in a sample containing 65% (v/v) glycerol and 0.1 M phosphate buffer, was less than 3; for stellacyanin, the ratio A(280 nm)/A(604 nm) under the same experimental conditions, was less than 7. Samples for spectrophotometric measurements contained approx. 1.2×10^{-4} M protein and 0.1 M phosphate buffer ($KH_2PO_4 + K_2HPO_4$, pH 7 in water at room temperature). Spectra were measured on protein aqueous solutions containing 65% (v/v) glycerol or ethylene glycol as cryoprotectants. These solutions remained homogeneous and transparent over the whole temperature range; indeed, no sample cracking was observed even at cryogenic temperatures, as confirmed also by the good quality of the baseline.

The experimental setup and methods used to measure optical absorption spectra in the temperature range 300–20 K have previously been described [5]. Experiments were performed with a Varian 2300 UV-Vis-near-infrared spectrophotometer controlled by an IBM PC; the spectrophotometer was operated in the 'constant gain' mode and the spectral bandwidth was less than 1.2 nm throughout the whole wavelength range investigated (1100–350 nm). The spectra were digitized with 2-nm steps; their deconvolution in terms of Gaussian components, $G(\nu) = A \exp(-(\nu - \nu_0)^2/2\sigma^2)$, was performed on an HP-1000 computer using a non-linear least-squares fitting algorithm. The quantity to be minimized in the fitting was $\chi^2 = \sum_j [A_j \text{ (observed)} - A_j \text{ (calculated)}]^2/(N - p)$ where $N = 375$ is the number of data points and $P = 12$ is the number of optimization parameters; all the data points in a spectrum were assumed to have the same experimental variance.

The temperature dependence of the baseline was determined by performing sets of measurements with solvent samples. No baseline variations were observed in the region 800–350 nm, in the whole temperature range; baseline variations were instead observed in the region 1100–800 nm, due to the absorption of the glycerol/water and ethylene glycol/water mixtures. The baseline measured at the same temperature was subtracted from each spectrum before analysis. The zeroth (M_0), first (M_1) and second (M_2) moment of each band were calculated within the narrow band approximation, according to the definitions given by Markham [1], i.e.,

$$M_0 = \int \epsilon(\nu)\, d\nu$$

$$M_1 = M_0^{-1} \int \nu \epsilon(\nu)\, d\nu$$

$$M_2 = M_0^{-1} \int \nu^2 \epsilon(\nu)\, d\nu - M_1^2$$

where $\epsilon(\nu)$ is the absorbance, at frequency ν, of the distribution that takes into account the band of interest.

3. Results

3.1. Azurin

Fig. 1. (left-hand panel) shows the optical absorption spectra of azurin in 65% (v/v) glycerol/water at various temperatures. The temperature-induced difference spectra are shown, on an expanded scale, in the right-hand panel of fig. 1. Absolute spectra and temperature-induced difference spectra obtained with samples in 65% (v/v) ethylene glycol/water are very similar to those reported in fig. 1. An increase of the central band at about 600 nm and a parallel decrease of the near-infrared band at about 850 nm that occur as the temperature is lowered are clearly demonstrated by the raw data in fig. 1.

The deconvolution of the measured spectra in Gaussian components is shown in fig. 2: four bands are identified and labeled I–IV in the figure. These bands are usually attributed to ligand to metal charge-transfer transitions; in particular, the scheme of orbital promotions proposed is as follows [11,12]: band I, πS (Cys) $\rightarrow$ $d_{x^2-y^2}$(Cu); band II, σS (Cys) $\rightarrow$ $d_{x^2-y^2}$(Cu); band III, σS (Met) $\rightarrow$ $d_{x^2-y^2}$(Cu); band IV, πN (His) $\rightarrow$ $d_{x^2-y^2}$(Cu). More recently a different assignment, based on low-temperature optical absorption and MCD and CD spectra in conjunction with self-consistent field scattered wave calculations, has been proposed by Gewirth and Solomon [13]; in their scheme band I would arise from a d-d transi-

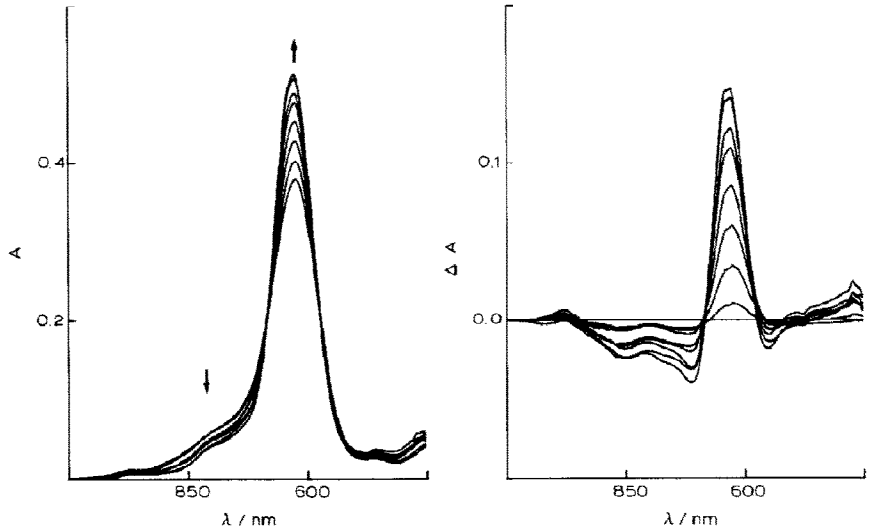

Fig. 1. (Left) Optical absorption spectra of azurin at $T = 260$, 230, 200, 170, 140, 110, 80 and 50 K. The arrows at about 850 and 600 nm indicate the direction of spectral changes observed on lowering the temperature. (Right) Temperature-induced difference spectra. $\Delta A(T)$ is defined as: $\Delta A(T) = A(T) - A(290\ \mathrm{K})$. All the spectra shown refer to samples in 65% (v/v) glycerol/water.

tion (although having a significant S (Cys) π mixing), band II from a πS (Cys) $\rightarrow d_{x^2-y^2}$(Cu) transition which becomes intensified by the extremely good overlap between the ground and excited state wave functions, band III from a pseudo σS (Cys) $\rightarrow d_{x^2-y^2}$(Cu) transition, while the assign-

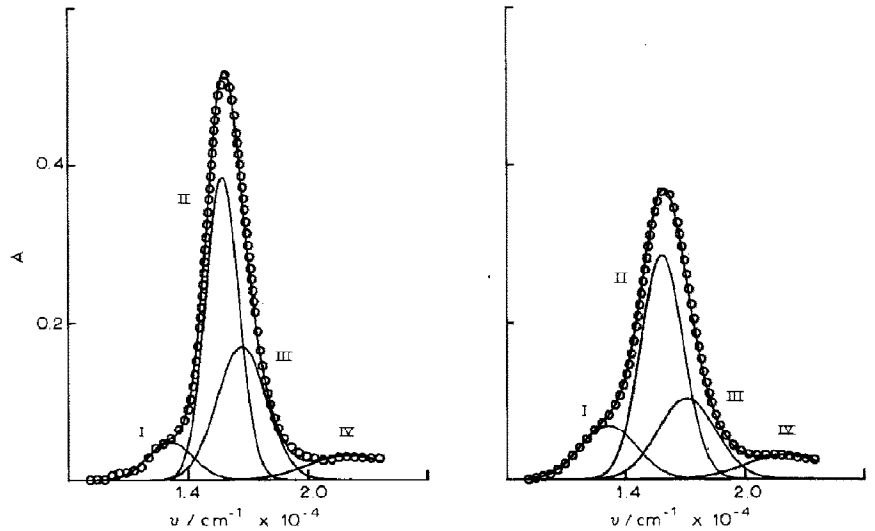

Fig. 2. Deconvolution of the absorption spectra of azurin in terms of gaussian components. (Left) $T = 20$ K; (right) $T = 290$ K. Spectra refer to samples in 65% (v/v) glycerol/water. (○) Experimental points; continuous lines represent the Gaussian components and the synthesized band profile. For the sake of clarity, not all of the experimental points have been reported. χ values (expressed in A units) are 8×10^{-3} at $T = 290$ K and 2×10^{-2} at $T = 20$ K.

ment of band IV remains unchanged. Concerning the deconvolutions reported in fig. 2 the following points are worth noting:

(i) Band IV is very small at all temperatures and not well defined, particularly on the high-frequency side; for these reasons it is not possible to make a meaningful analysis of its temperature dependence. Moreover, to avoid possible artifacts arising from its mixing with the central band, M_1 and M_2 values of Gaussian component IV are determined from low-temperature spectra and imposed constant in the whole temperature range.

(ii) Bands II and III are not resolved separately, even at low temperatures. For this reason we consider a single band arising from the sum of bands II and III; the moments of this band are calculated from the distribution resulting from the sum of the Gaussian components II and III.

(iii) Band I appears as a shoulder on the low-frequency side of the central band; at high

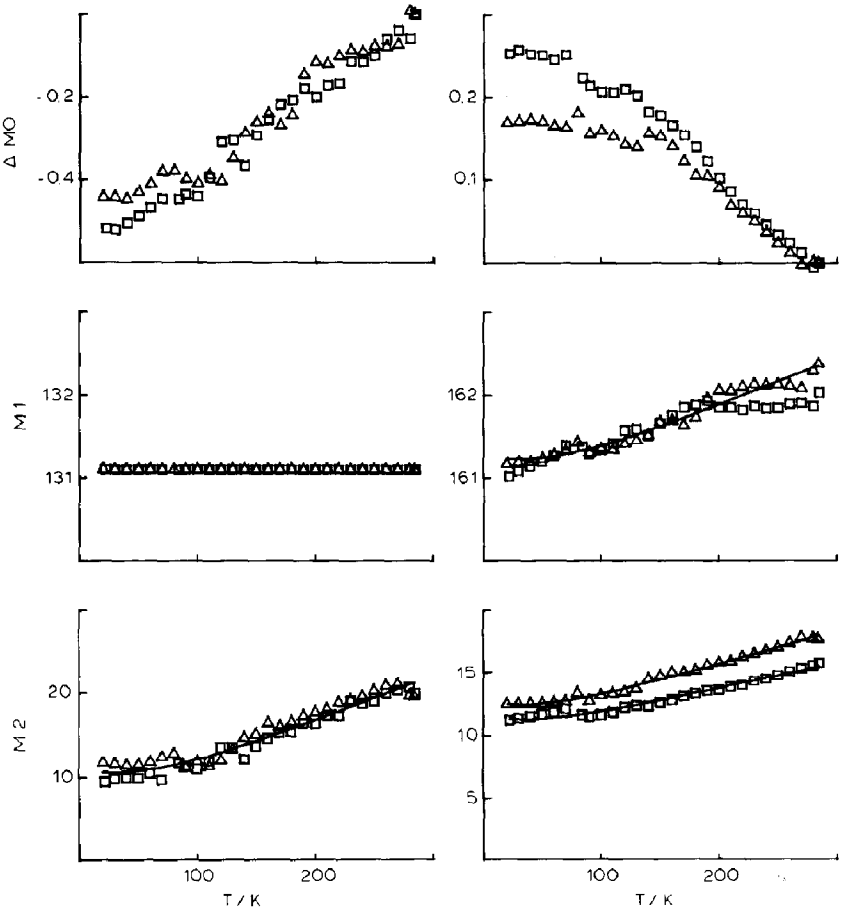

Fig. 3. ΔM_0, M_1 and M_2 relative to the optical absorption bands of azurin as a function of temperature. (Left) Band I; (right) band II + III. ΔM_0 is defined as $\Delta M_0 = M_0(T)/M_0(290\ \mathrm{K}) - 1$. Samples in: (△) 65% glycerol/water; (□) 65% ethylene glycol/water. Continuous lines represent the best fit of eqs 2 to the experimental points. For M_1 values relative to band II + III, the fitting refers to points in 65% glycerol/water only. The M_1 scale is in units of $\mathrm{cm}^{-1} \times 10^{-2}$; the M_2 scale is $\mathrm{cm}^{-2} \times 10^{-5}$.

Table 1

Values of the parameters obtained by fitting M_1 and M_2 of the optical absorption bands of azurin in terms of eqs 2

Band	Solvent	A ($\mu^{-2}\times10^4$)	ν (cm^{-1})	C ($\mu^{-1}\times10^2$)	D (μ^{-1})	F ($\mu^{-1}\times10^2$)
I	65% glycerol/water	57 ± 16 [a]	150 ± 25	$7\ \pm1$	1.311	0
I	65% ethylene glycol/water	57 ± 16 [a]	150 ± 25	$7\ \pm1$	1.311	0
II + III	65% glycerol/water	31 ± 5	150 ± 15	9.6 ± 0.2	1.606 ± 0.001	0.62 ± 0.2
II + III	65% ethylene glycol/water	23 ± 6	150 ± 25	9.5 ± 0.3	– [b]	– [b]

[a] In view of the fact that for band I solvent effects are almost absent, these parameters values are obtained by fitting together M_2 values relative to both solvents. Values of the standard deviations are obtained directly from the fittings. Standard deviations relative to parameters D and F of band I are not given since M_1 values relative to this band have been imposed constant in the fitting procedure.

[b] For M_1 values relative to band II + III in 65% ethylene glycol/water the fitting has not been performed (see text).

temperatures, due to an increase in the width, the shoulder is less well resolved and tends to merge into the central band. To avoid artifacts in the analysis of the high-temperature spectra, the M_1 value (i.e., the peak position) of Gaussian component I is determined from the low-temperature spectra (20–160 K) and imposed constant at all temperatures.

In fig. 3 we report the values of ΔM_0 (i.e., the fractional M_0 variation with respect to its high-temperature value), M_1 and M_2 relative to band I and II + III as a function of temperature. Lowering the temperature from 290 to 20 K causes an integrated intensity decrease of about 50% for band I and an increase of about 20% for band II + III. The temperature dependence of M_1 and

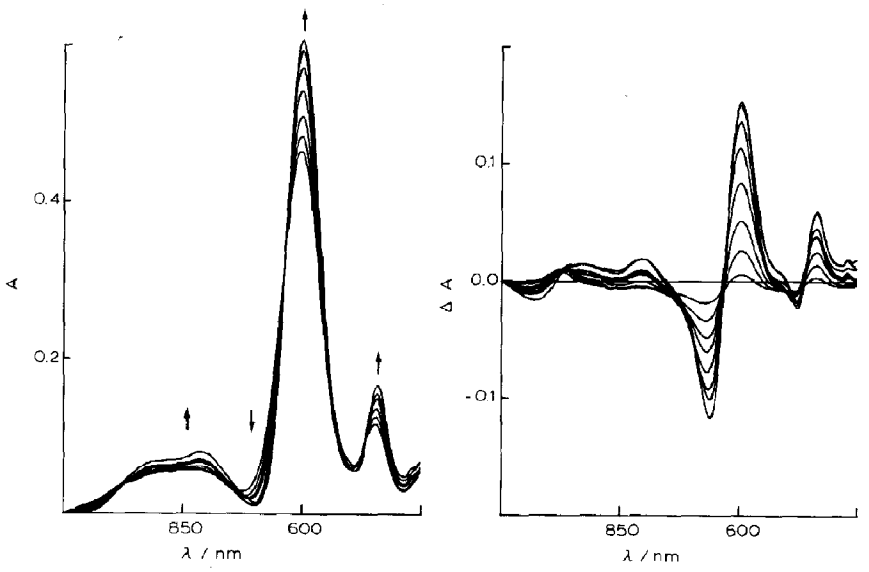

Fig. 4. (Left) Optical absorption spectra of stellacyanin at $T = 260$, 230, 200, 170, 140, 110 and 80 K. The arrows at about 850, 700, 600 and 450 nm indicate the direction of spectral changes observed on lowering the temperature. (Right) Temperature-induced, difference spectra. The data refer to samples in 65% (v/v) ethylene glycol/water.

M_2 relative to both bands is in agreement with eqs 2, except for small deviations observed at high temperatures in the behavior of M_1 values relative to band II + III; these deviations are larger when 65% ethylene glycol/water is used as solvent. For this reason the M_1 fitting reported in fig. 3 for band II + III refers to points in 65% glycerol/water only. The values of the parameters obtained by fitting M_1 and M_2 with eqs 2 are reported in table 1. The effects of solvent composition on the thermal behavior of M_1 and M_2, although systematically present, are very small; in particular, it should be noted that identical values of the parameter ν (150 cm^{-1}) are obtained in the two different solvents.

3.2. Stellacyanin

The optical absorption spectra of stellacyanin at various temperatures and the temperature-induced difference spectra are shown in fig. 4. The data refer to samples in 65% glycerol/water; the behavior in 65% ethylene glycol/water is similar. In analogy with azurin, an increase in the central band at about 600 nm is observed by lowering the temperature; in contrast to azurin, the band at about 850 nm also increases as the temperature is lowered.

The deconvolution of the measured spectra into Gaussian components is shown in fig. 5 and is analogous to that reported above for azurin. The four bands observed are usually attributed to ligand-metal charge-transfer transitions and the scheme of orbital promotions proposed is as follows: band I, πS (Cys) $\rightarrow$ $d_{x^2-y^2}$(Cu); band II, σS (Cys) $\rightarrow$ $d_{x^2-y^2}$(Cu); band III, σS (Cystine) $\rightarrow$ $d_{x^2-y^2}$(Cu); band IV, πN (His) $\rightarrow$ $d_{x^2-y^2}$(Cu). Also for stellacyanin a different assignment has been recently proposed, in analogy with azurin and plastocyanin. Concerning the deconvolution reported in fig. 5, the following aspects deserve mentioning:

(i) A straight line tangent to the minima at about 1100 nm and at about 390 nm (see fig. 4) is first subtracted as a baseline from the experimental spectra. The spectra and the

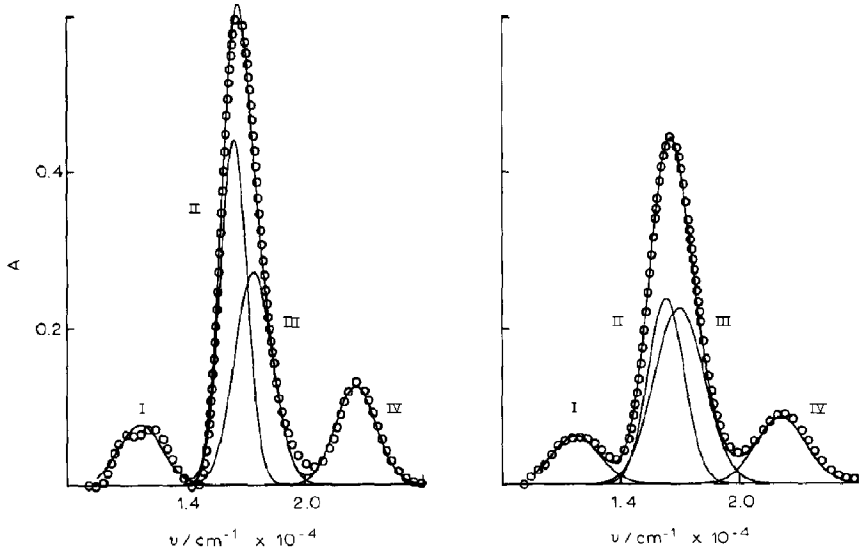

Fig. 5. Deconvolution of the absorption spectra of stellacyanin in terms of Gaussian components. (Left) $T = 20$ K; (right) $T = 290$ K. Spectra refer to samples in 65% ethylene glycol/water. Symbols as in fig. 2. χ values (expressed in A units) are 2×10^{-2} at $T = 290$ K and 8×10^{-2} at $T = 20$ K. Note that, before performing the deconvolution, a straight line tangent to the minima at about 1100 and 390 nm has been subtracted from the raw spectra.

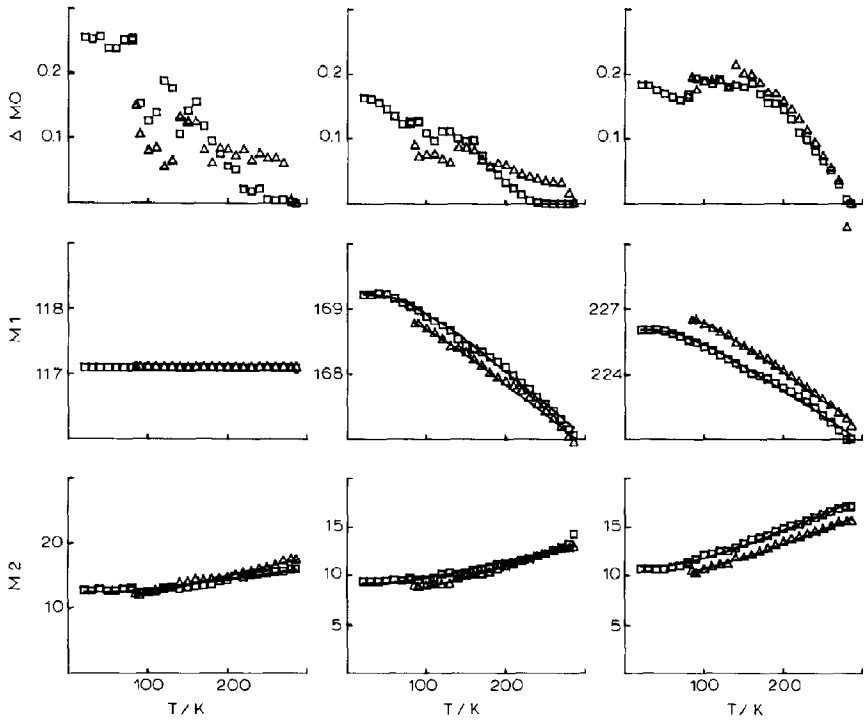

Fig. 6. ΔM_0, M_1 and M_2 relative to the optical absorption bands of stellacyanin as a function of temperature. (Left) Band I; (center) band II + III; (right) band IV. Symbols and scales as in fig. 3. The continuous lines represent the best fit of eqs 2 to the experimental points.

deconvolutions reported in fig. 5 have been obtained by this procedure.

(ii) In contrast to azurin, band IV of stellacyanin is very well defined at all temperatures and therefore the temperature dependence of its moments is analyzed in detail.

Table 2

Values of the parameters obtained by fitting M_1 and M_2 of the optical absorption bands of stellacyanin in terms of eqs 2

Band	Solvent	A ($\mu^{-2}\times10^4$)	ν (cm^{-1})	C ($\mu^{-1}\times10^2$)	D (μ^{-1})	F ($\mu^{-1}\times10^2$)
I	65% glycerol/water	35 ± 15 [a]	160 [b]	9 ± 0.7	1.171	0
I	65% ethylene glycol/water	21 ± 8	160 ± 30	10 ± 0.4	1.171	0
II + III	65% glycerol/water	30 ± 15	160	7 ± 0.9	1.701 ± 0.002	-1.1 ± 0.3
II + III	65% ethylene glycol/water	24 ± 8	160 ± 30	8 ± 0.4	1.704 ± 0.001	-1.2 ± 0.1
IV	65% glycerol/water	36 ± 9	160	8 ± 0.5	2.302 ± 0.002	-3.1 ± 0.6
IV	65% ethylene glycol/water	39 ± 6	160 ± 15	8 ± 0.3	2.289 ± 0.001	-2.9 ± 0.4

[a] Values of the standard deviations are obtained directly from the fittings. Standard deviations relative to parameters D and F of band I are not reported, since M_1 of this band is imposed constant in the fitting procedure.

[b] In the fitting of M_1 and M_2 relative to samples in 65% glycerol/water, the ν values have been taken to be equal to those obtained from samples in 65% ethylene glycol/water, since the reduced temperature interval does not enable one to perform an independent and meaningful evaluation of this parameter.

(iii) In analogy with azurin, bands II and III are not resolved separately. We therefore consider a single band arising from their sum; the moments of this band are calculated from the distribution resulting from the sum of the Gaussian components II and III.

(iv) At low temperatures, band I is well resolved and appears to be split into two components; however, as the temperature increases, this band is poorly resolved (see fig. 4) and tends to merge into the central band. To avoid artifacts in the analysis of high-temperature spectra a single Gaussian component is taken to account for band I; moreover, in analogy with azurin its M_1 value is determined from the low-temperature spectra (20–150 K) and imposed constant at all temperatures.

Fig. 6 shows the values of ΔM_0, M_1 and M_2 relative to bands I, II + III and IV as a function of temperature. The integrated intensities of all bands increase by about 20% as the temperature is lowered from 290 to 20 K. The temperature dependence of M_1 and M_2 relative to all bands is in agreement with eqs 2; the values of the fitting parameters are reported in table 2. Concerning the effects of solvent composition, they are small for bands I and II + III and sizably larger for both M_1 and M_2 relative to band IV. It should be noted that, for stellacyanin, measurements in 65% glycerol/water are limited to the temperature range 80–290 K; this range is not sufficiently wide for a meaningful determination of the parameter ν. In view of the fact that (i) for azurin, identical ν values are observed in the two solvents and (ii) for stellacyanin, the ν values in 65% ethylene glycol/water are almost identical to those relative to azurin, the value of the parameter ν is fixed to 160 cm^{-1} in the fitting of M_1 and M_2 values in 65% glycerol/water.

4. Discussion

The data shown in figs 3 and 6 clearly show that the integrated intensities (M_0 values) of all the observed bands vary as the temperature is lowered. These variations (also evident in the raw spectra, see figs 1 and 4) are large (about 20–30% or even greater) and can be either positive or negative; for these reasons they cannot be attributed either to variations of the sample volume due to thermal contraction or to artifacts arising from the deconvolution procedure.

In the case of charge-transfer bands, integrated intensity variations are readily interpretable as being due to differing degrees of overlap between the molecular orbitals involved in the electronic transitions that give rise to the absorption bands. For azurin and stellacyanin, this would imply that the overlap between the copper and ligand orbitals involved in the charge-transfer transitions is temperature-dependent; variations of the metal-ligand relative positions, i.e., deformations of the active site, therefore occur as the temperature is varied. For bands arising from d-d transitions the above mechanism is obviously inapplicable. Our data relative to band I, however, are not inconsistent with the assignment reported in ref. 13, since the d-d transition that gives rise to this band is suggested to have significant S (Cys) π mixing.

Concerning M_1 and M_2, the data in figs 3 and 6 show that their temperature dependence can be well rationalized in terms of eqs 2. One likely exception might be the behavior of the first moment of band II + III of azurin in 65% ethylene glycol/water, where a deviation from the predictions of eq. 2a is observed at temperatures higher than about 190 K. Analogous (although much more dramatic) deviations, present in the behavior of M_1 but not in that of M_2, have already been observed for the visible bands of liganded ferrous myoglobin [7] and have been attributed to a conformational readjustment of the protein that takes place following the solvent glass transition and that alters the electric field 'seen' by the electron that undergoes the optical transition without substantially altering either the frequency of nuclear motions or their coupling constants with the electronic transitions.

The data listed in tables 1 and 2 show that the mean effective frequency of the nuclear motions coupled with the electronic transitions (ν) is about 150 cm^{-1} both for azurin and for stellacyanin;

this value depends neither upon the particular band considered nor upon the solvent composition. Two previous investigations from other laboratories reported ν values of about 350 cm^{-1} [11] and about 35 cm^{-1} [14]. The former value was obtained from the temperature dependence of optical spectra measured in thin films of dried proteins; however, the data points relative to only four temperatures (i.e., 35, 60, 120 and 200 K) were consider in the analysis. The latter value was obtained from the temperature dependence of $g_{\parallel}$ values measured from EPR spectra; the experimental data, however, were available only in the range 77–200 K, where linear behavior of $g_{\parallel}$ with temperature was observed. Concerning the latter data, when comparing data from optical and EPR spectroscopy, it must be borne in mind that, since different kinds of electronic transitions are involved, the interactions with nuclear vibrations could also be different. Since the ν values are obtained by averaging over the normal modes weighted with their coupling constants (see, e.g., eqs 1a and 1b), different ν values could in principle be recorded with two experimental techniques.

In order to compare in greater detail our results with those mentioned above, we performed the fittings reported in fig. 7. In the top panel of fig. 7, the M_1 values of band II + III of stellacyanin are reported as a function of temperature. The data points at 30, 60, 120 and 200 K are marked by arrows and the solid line is a best fit of eq. 2a to the above four experimental points whereby the ν value is held fixed at 350 cm^{-1}. It is evident that although the solid line fits the four points reasonably well, a systematic overall misfit is present. In the center panel of fig. 7, the M_1 values in the range 80–200 K are delimited by arrows and the solid line is a best fit to the data points in this temperature range whereby the ν value is held fixed at 35 cm^{-1}; once again the solid line fits the data points concerned quite well, whereas a systematic misfit to the overall M_1 behavior is evident. The fitting performed in this work on the whole set of experimental data (yielding a ν value of 160 cm^{-1}) is reported in the bottom panel of fig. 7, for the sake of comparison. Inspection of fig. 7 indicates that, to achieve a correct determination of ν values, a large number of experimental data over the widest temperature range attainable are needed.

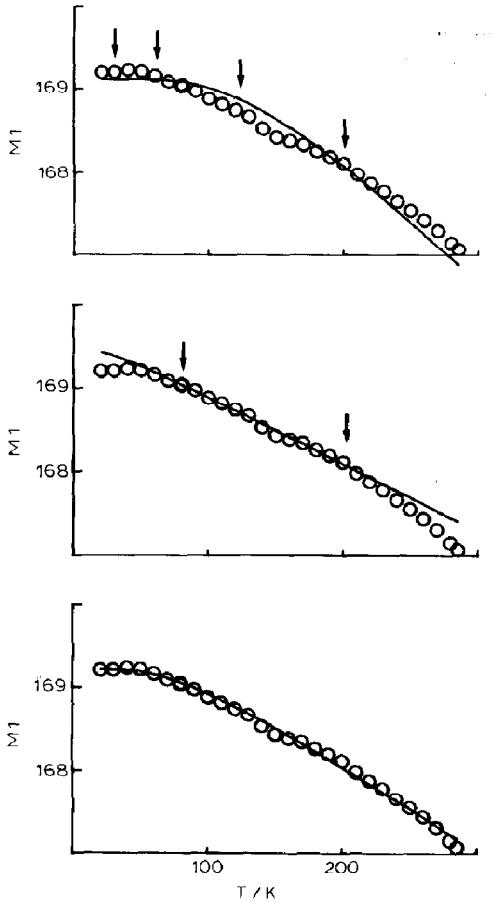

Fig. 7. (Top) M_1 values ($cm^{-1} \times 10^{-2}$) relative to band II+III of stellacyanin as a function of temperature. Data points at 30, 60, 120 and 200 K are marked by arrows. The solid line is a best fit of eq. 2a to the above data points with the value of the parameter ν held constant at 350 cm^{-1}. (Center) Same as in the top panel. The range 80–200 K is delimited by arrows. The solid line is a best fit of eq. 2a with the value of the parameters ν held constant at 35 cm^{-1}. (Bottom) Same experimental data as in top and center panels. The solid line is a best fit of eq. 2a to the whole set of experimental data and yields a ν value of 160 cm^{-1}.

In agreement with the data in ref. 11, the spectra of azurin and stellacyanin do not exhibit any vibronic structure, even at 20 K. This fact implies that the ν value of 150 cm^{-1} results from the weak coupling of the electronic transitions

with several vibrational modes whose 'mean effective' frequency (weighted over the coupling constants) is about 150 cm^{-1} rather than from a strong coupling with a single (or few) vibrational mode(s).

In the resonance Raman spectra of blue copper proteins [15–18], intense bands are observed near 400 cm^{-1} and are assigned to Cu-ligand stretching motions; weaker bands are also evident in the range 120–170 cm^{-1} and are attributed to ligand-Cu-ligand deformations and/or to ligand torsion. Our data show that the optical bands of azurin and stellacyanin are substantially coupled with low-frequency modes: the above-mentioned deformation modes are likely to be involved.

Another interesting point to emerge from the data listed in tables 1 and 2 is the systematic presence of large C values. As mentioned in section 1, non-zero C values can originate via three different physical mechanisms, i.e., homogeneous broadening, due to the finite lifetime of the excited electronic state, inhomogeneous broadening, due to the presence of a spectrally heterogeneous ensemble of protein molecules, and coupling with high-frequency vibrational modes that are populated only at the zero-point level in the temperature range investigated. Our data do not enable us to distinguish between these three contributions; however, it is tempting to speculate that, in agreement with the suggestion in the literature that azurin exhibits conformational heterogeneity [19,20], inhomogeneous broadening substantially contributes to the large C values shown in tables 1 and 2. The relevance of inhomogeneous broadening to the width of the visible bands of the carbonmonoxy derivatives of sperm whale myoglobin and of isolated hemoglobin α- and β-subunits has also been recently suggested (E.E. Di Iorio et al., manuscript in preparation).

Concerning the effect of solvent composition on the temperature dependence of the absorption bands, the data in figs 3 and 6 show that a solvent effect on M_1 and M_2 is indeed observed. However, in view of the smallness of the effect as compared to the standard deviations of the values of our parameters (see tables 1 and 2), it is not possible to draw any quantitative conclusion from these data.

We wish now to speculate on the possible functional significance of our results. Ligand-metal-ligand deformation modes at about 150 cm^{-1} are significantly populated at room temperature ($kT = 215$ cm^{-1} at 300 K). Our data indicate that these low-frequency local modes are coupled with the electronic transitions and therefore particularly with the copper $d_{x^2-y^2}$ orbital that, in turn, is directly involved in the biological functions of these proteins. A direct role of these low-frequency modes on the electron-transfer process can therefore be suggested.

A second point of possible functional interest is the M_0 variation with temperature shown in figs 3 and 6. As already discussed, this effect is interpreted in terms of variations of the copper-ligand relative positions (i.e., deformations of the active site) that occur as the temperature is lowered. Active site deformations, induced, for example, by the binding of heterotropic ligands and/or of other proteins, could be relevant in regulating the screening of the $d_{x^2-y^2}$ orbital by the endogenous ligands [21] and therefore the electron transfer to/from the orbitals of the redox partners.

More data are needed in order to substantiate the above speculations; in particular, a comparative study of several blue copper proteins and a correlation of their stereodynamic and functional (e.g., redox potentials) properties appear promising.

Acknowledgements

We are particularly indebted to Professor B. Salvato for his kind gift of the stellacyanin sample. The technical help of Mr G. Lapis and Mr M. Quartararo is also gratefully acknowledged. This work has been supported also by MPI 60% and CRRNSM grants.

References

1 J.J. Markham, Rev. Mod. Phys. 31 (1959) 956.
2 Y. Farge and M.P. Fontana, Electronic and vibrational properties of point defects in ionic crystals (North-Holland, Amsterdam, 1979).

3 G. Baldini, E. Mulazzi and N. Terzi, Phys. Rev. 140 (1965) 2094.
4 K.T. Schomacker and P. Champion, J. Chem. Phys. 84 (1986) 5314.
5 L. Cordone, A. Cupane, M. Leone and E. Vitrano, Biophys. Chem. 24 (1986) 259.
6 M. Leone, A. Cupane, E. Vitrano and L. Cordone, Biopolymers 26 (1987) 1769.
7 L. Cordone, A. Cupane, M. Leone, E. Vitrano and D. Bulone, J. Mol. Biol. 199 (1988) 213.
8 A. Cupane, M. Leone, E. Vitrano and L. Cordone, Biopolymers 27 (1988) 1977.
9 E.T. Adman, in: Metalloproteins, part 1, ed. P. Harrison (Verlag Chemie, Weinheim, 1985) p. 1.
10 B. Reinhammar, Biochem. Biophys. Acta 205 (1970) 35.
11 E.I. Solomon, J.W. Hare, D.M. Dooley, J.H. Dawson, P.J. Stephens and H.B. Gray, J. Am. Chem. Soc. 102 (1980) 168.
12 D.R. McMillin and M.C. Morris, Proc. Natl. Acad. Sci. U.S.A. 78 (1981) 6567.
13 A.A. Gewirth and E.I. Solomon, J. Am. Chem. Soc 110 (1988) 3811.
14 M. Bacci and S. Cannistraro, Chem. Phys. Lett. 133 (1987) 109.
15 W.H. Woodruff, K.A. Norton, B.I. Swanson and H.A. Fry, Proc. Natl. Acad. Sci. U.S.A. 81 (1984) 1263.
16 L. Nestor, J.A. Woolery, B. Reinhammar and T.G. Spiro, Biochemistry 23 (1984) 1084.
17 E.W. Ainscough, A.G. Bingham, A.M. Brodie, W.R. Ellis, H.B. Gray, T.M. Loehr, J.E. Plowman, G.E. Norris and E.N. Baker, Biochemistry 26 (1987) 71.
18 Y. Mino, T.M. Loehr, K. Wada, H. Matsubara and J. Sanders-Loehr, Biochemistry 26 (1987) 8059.
19 C.M. Hutnik and A.G. Szabo, Biochemistry 28 (1989) 3923.
20 E. Gratton, N. Silva and S. Ferreira, in: Biological and artificial intelligence systems, eds E. Clementi and S. Chin (Escom, Leiden, The Netherlands, 1988) p. 49.
21 Y. Nishida, Z. Naturforsch. 42c (1987) 1358.